Other subjects before Lesson III

Data for Other materials

Sn, W, SS304, Mo, Fe,…

$X=R_p/R_s$, $Y= (I_3-I_4)/(I_3+I_4)$ trajectories are similar with different pump intensity.

Pump intensity changed from $I=2\times10^{13}W/cm^2 \sim 4\times10^{12}W/cm^2$.

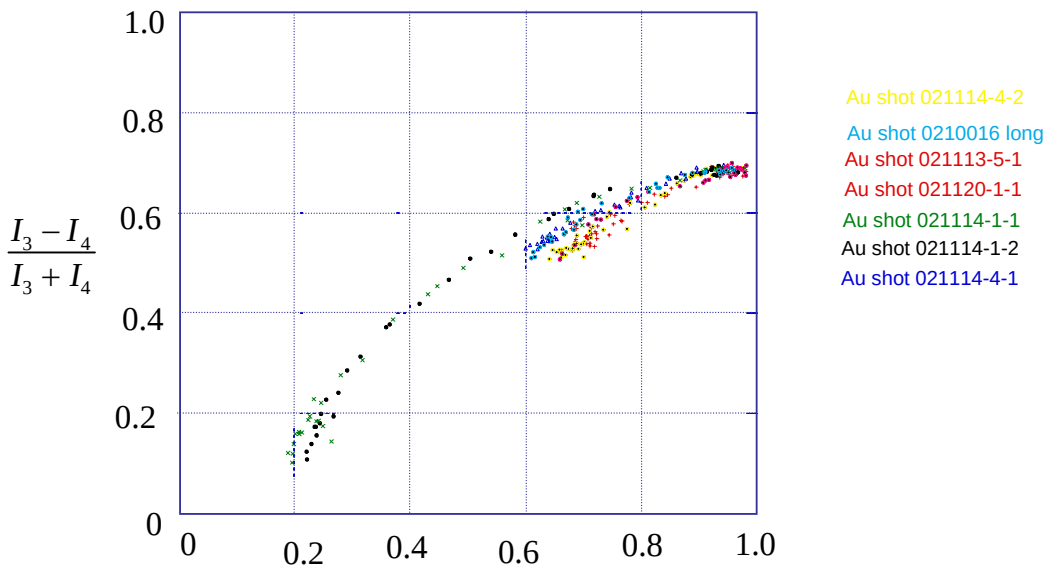

→ Expansion component was the same ion abundance.
==>Neutral Au!

Pump intensity dependence of Sn target.

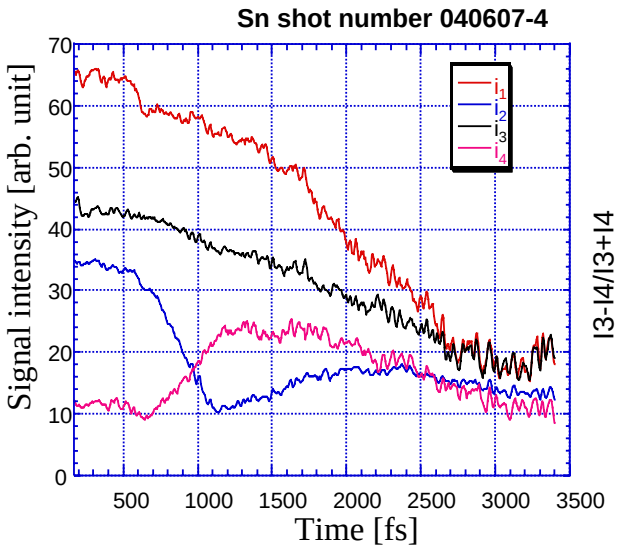

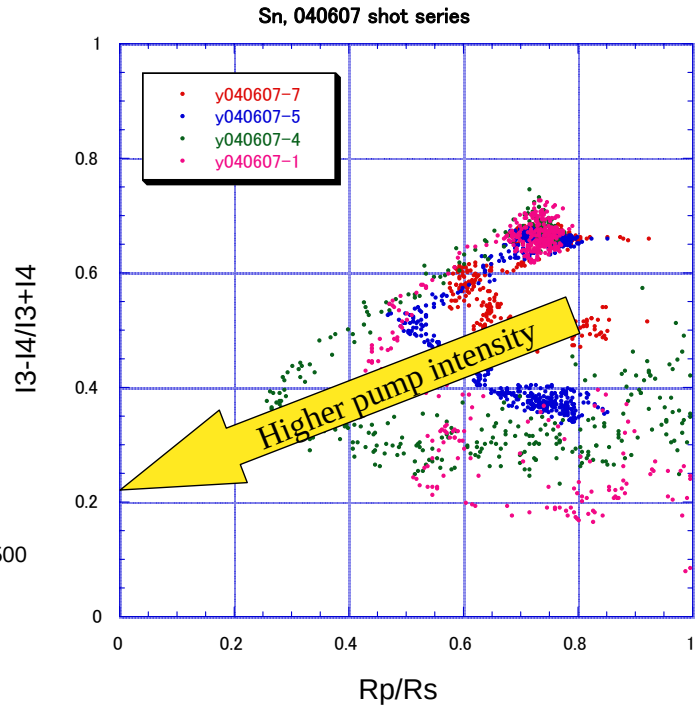

Three stages for Sn

a. Warm solid density plasma
b. + expansion warm dense gas
c. + cooling dense gas & droplets

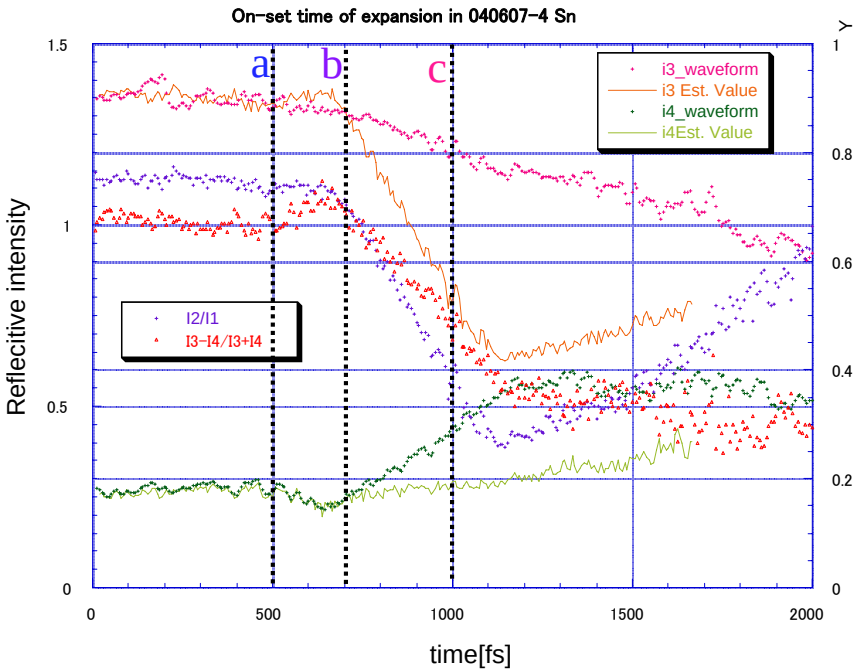

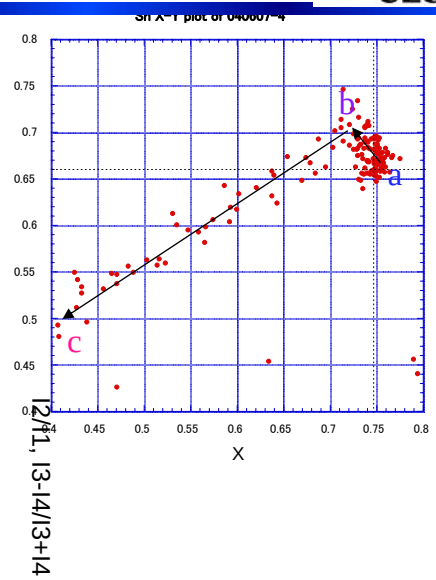

Comparison between SS304 and Fe.

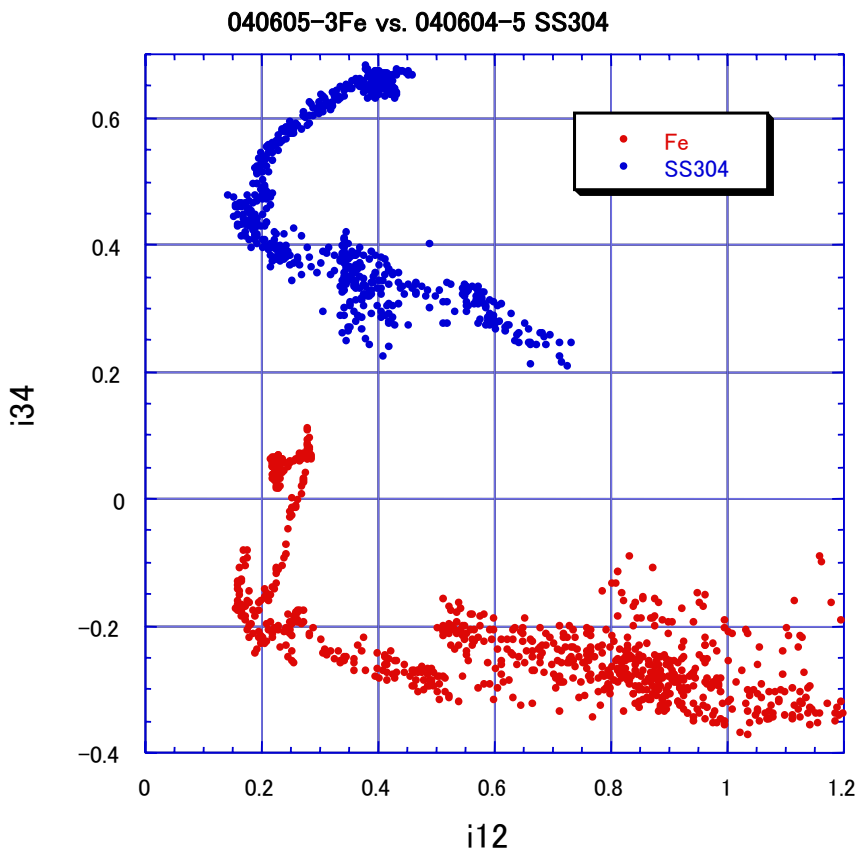

Evidence of touching two fluid region

The way to detect the unknown critical points

Diffused scattering detection

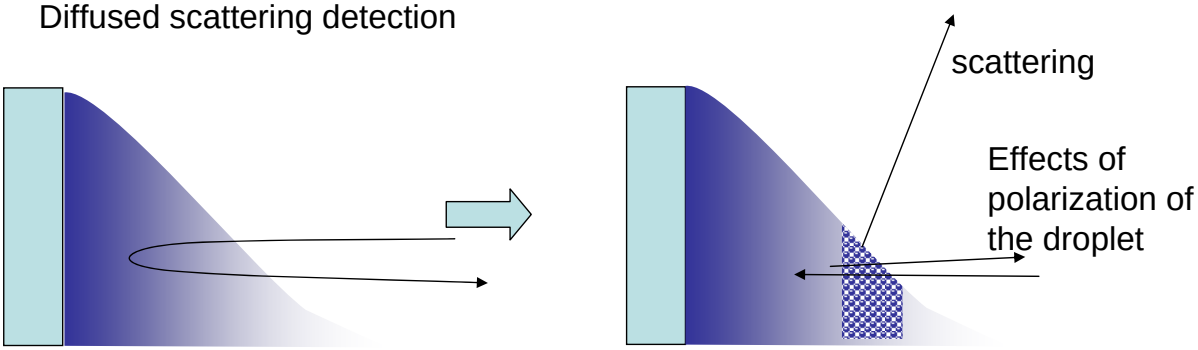

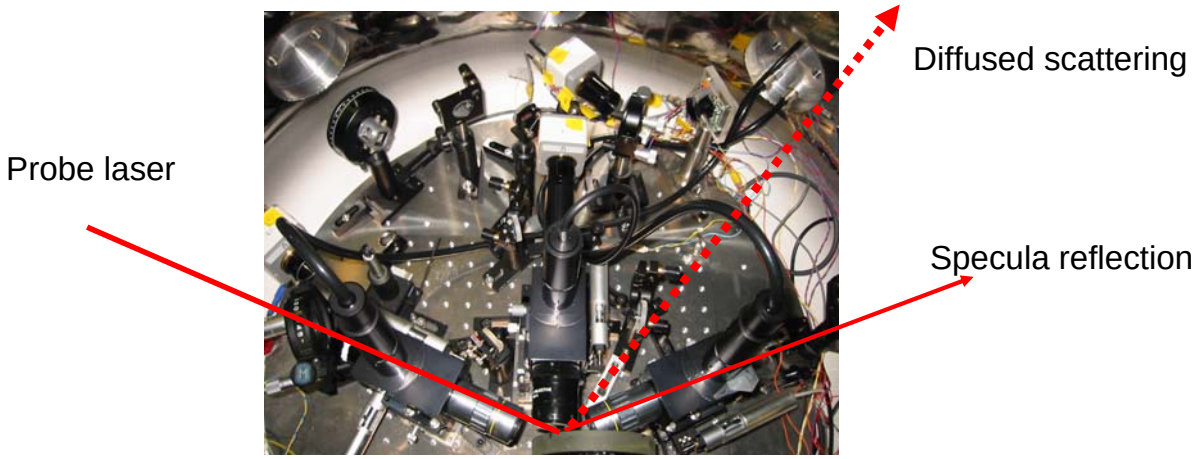

Time required to form droplets (expansion time + formation time)

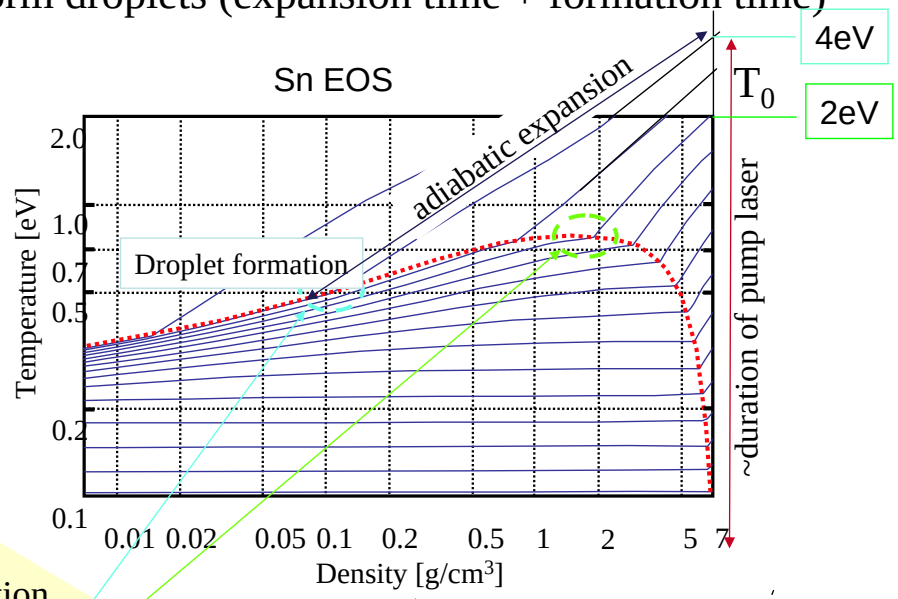

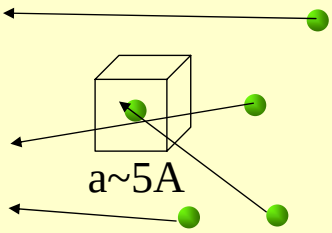

Rate of droplet formation

$$\frac{1}{R_{droplet}} = v_{atom} \cdot n_{atom} \cdot a^2 = 1.6 \times 10^{12} [s^{-1}]$$

$$6.3 \times 10^{10}$$

ρ=1.5g/cc, T=0.8eV
$t_{formation}$~600fs

ρ=0.1g/cc, T=0.5eV
$t_{formation}$~16ps

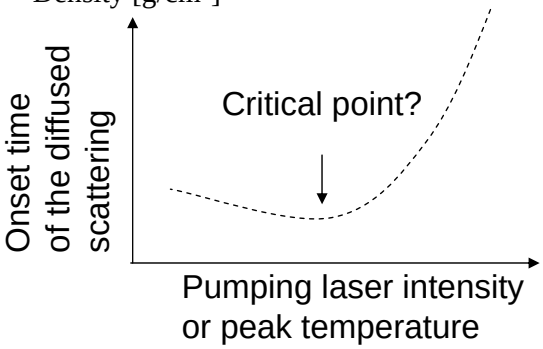

Detection of 2ϕ fluid with diffuse scattering signals

Au 0.6~2.6ps

W 0.75~1ps

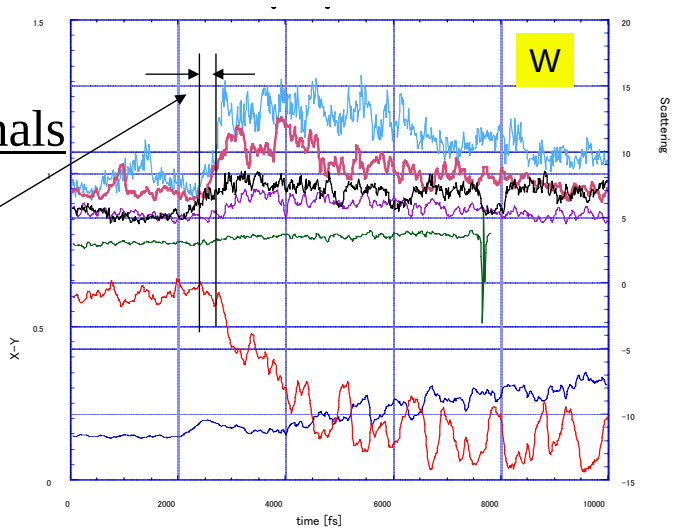

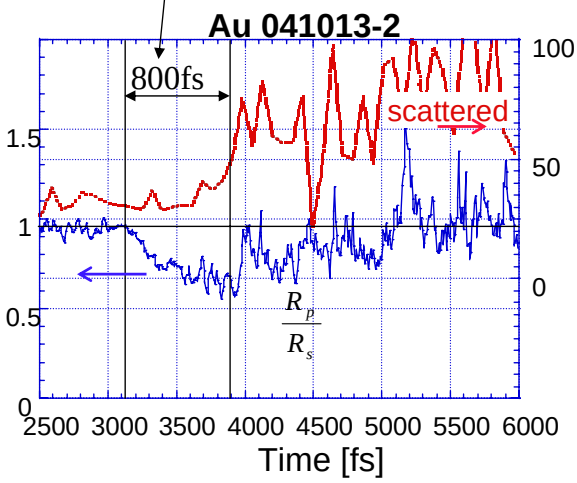

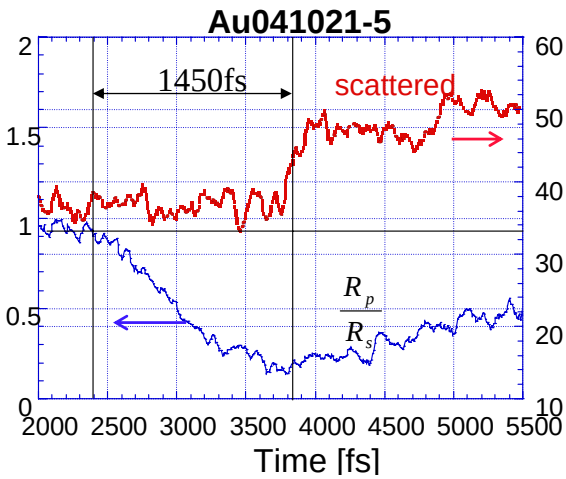

Droplet particles may have some contribution to the ellipsometric data.

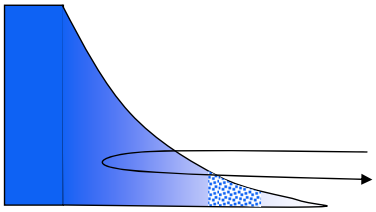

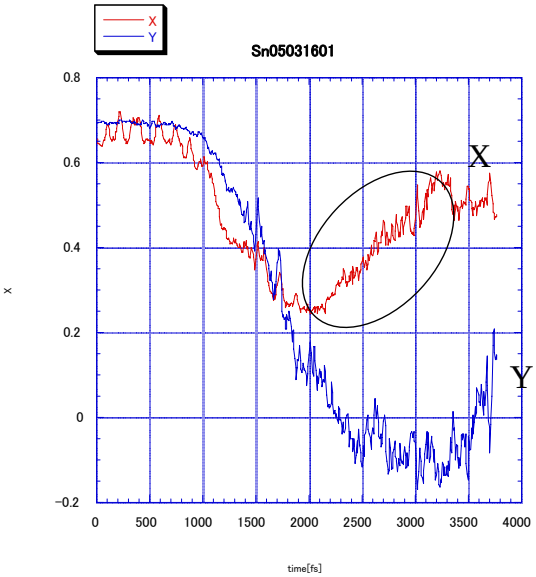

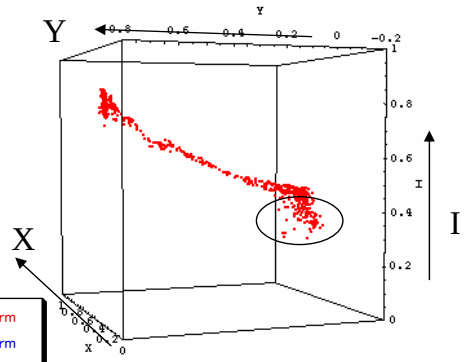

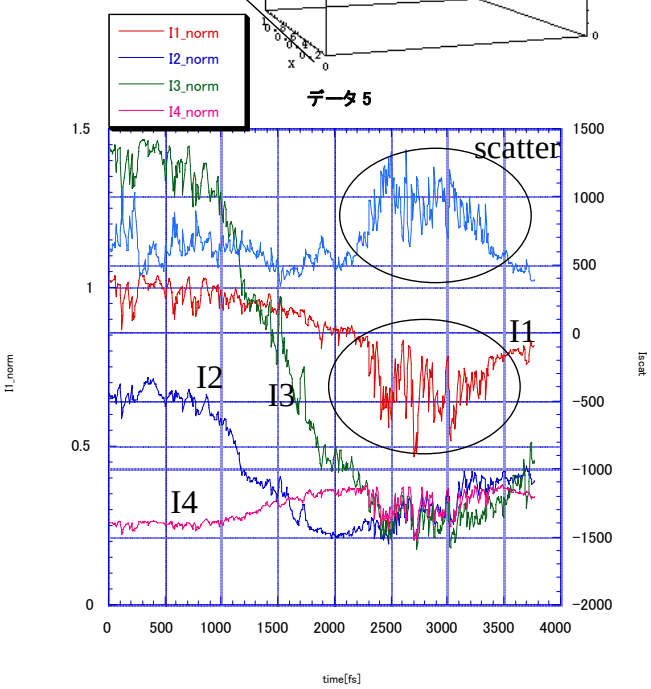

Evidence of negative –positive ions plasma

Emission from recombination

Electrons captured by neutrals

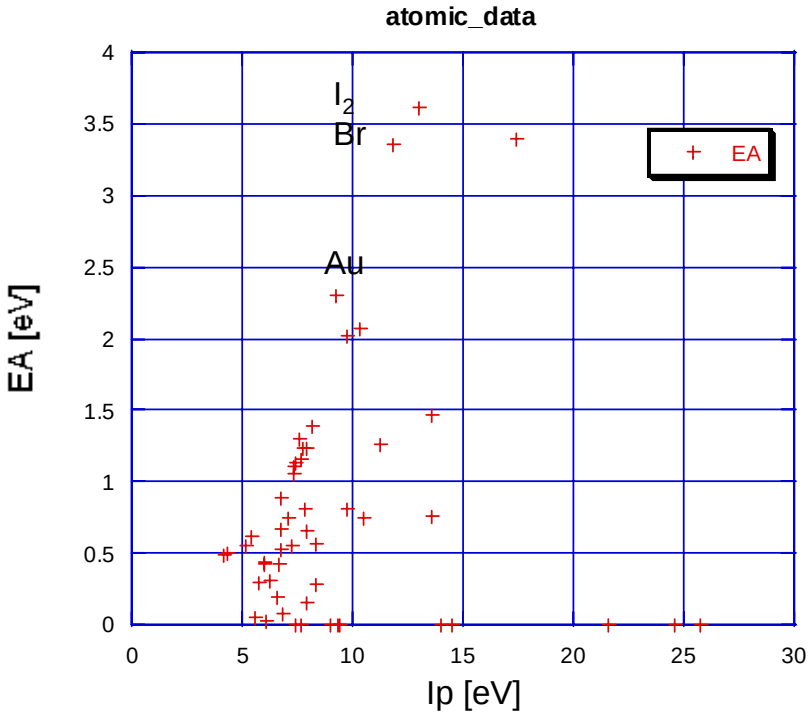

from R.M.More

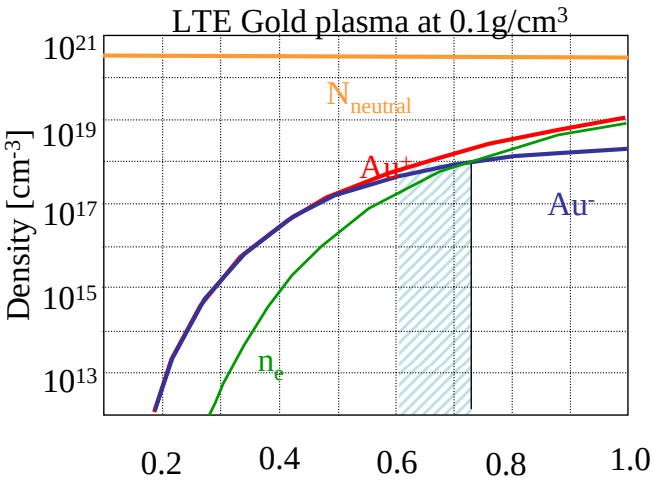

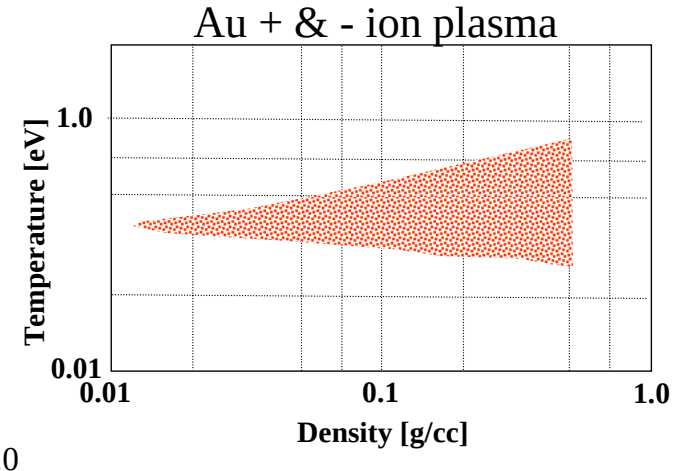

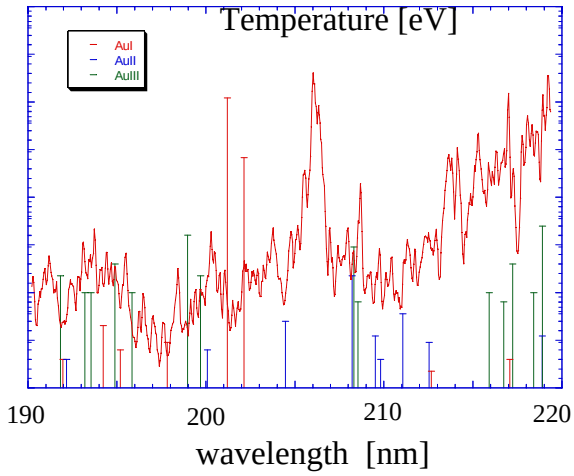

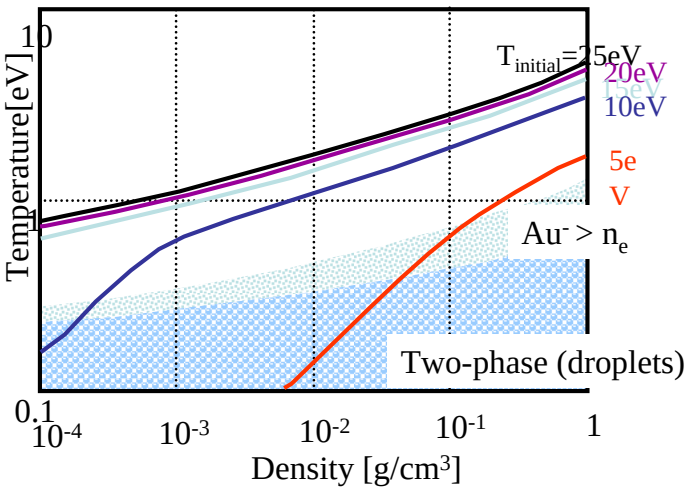

Lesson III
Laser Experiments

Next step toward further understanding

Plasma photonic device:

Mechanism of Reflectivity change

- If we assume Drude-like metalic material,

  Required energy ~ ionization potential

  1st Ionization potential for Hg =10.437eV =>340mJ/cm^2

- If we use M-NM transition,

  Required energy ~ transit temperature * specific heat

  Cp=27J/K/mol for Hg => 12mJ/cm^2

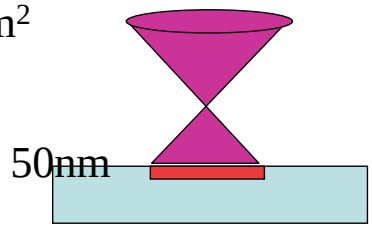

<u>Threshold intensity, dR/R, Speed of switching</u>

Why WDM physics? (3)

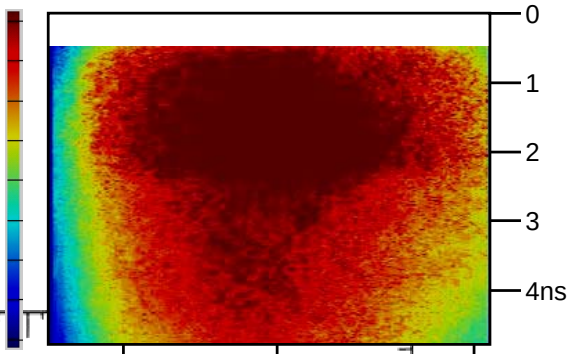

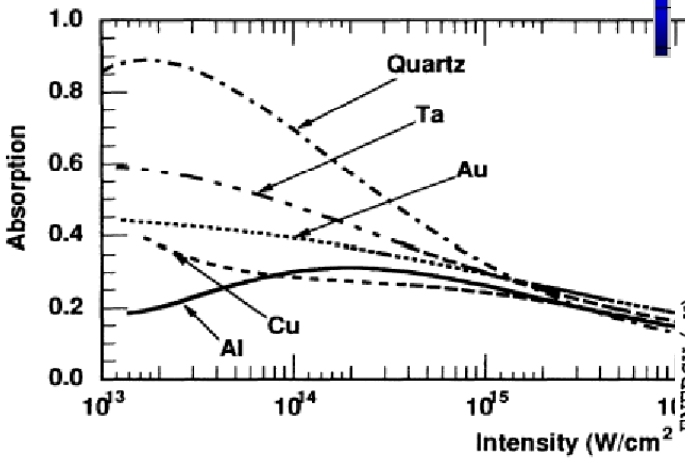

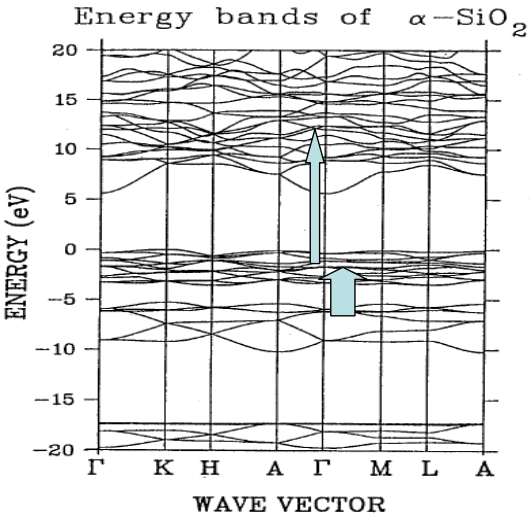

Warm dense matter

This Al properties can be explained by Drude law

D.F.Price, et al.,PRL, Vol.75-2, 252 (1995)

Metal-Nonmetal transition in Hg

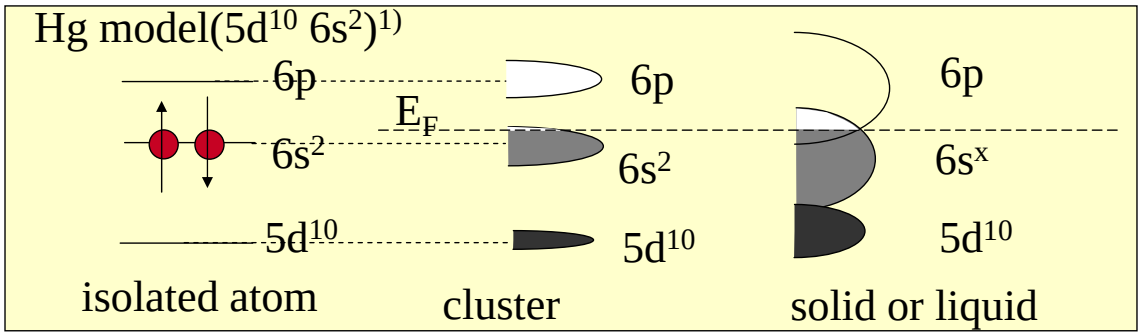

1)H. Haberland, et al., PRL, vol.69, p.3212

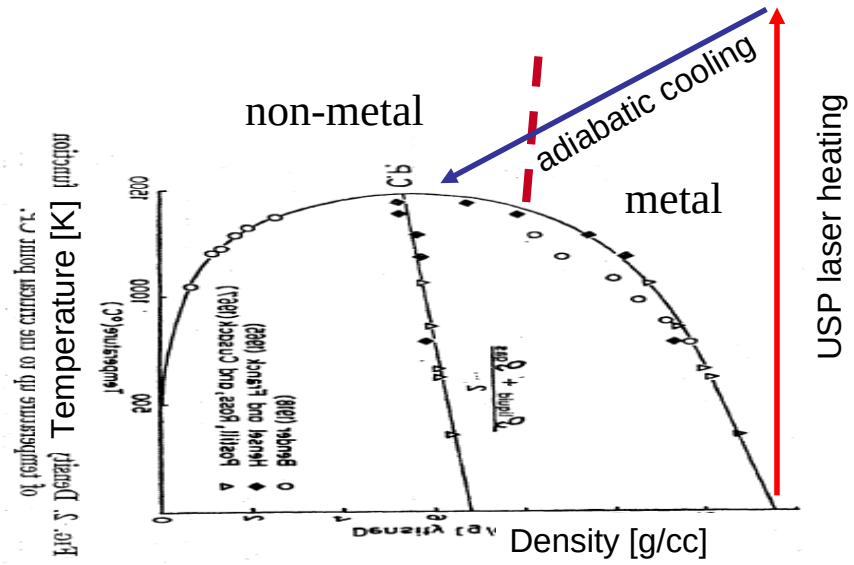

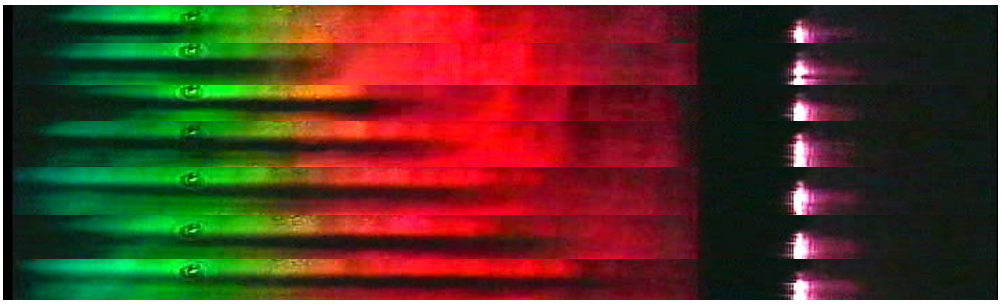

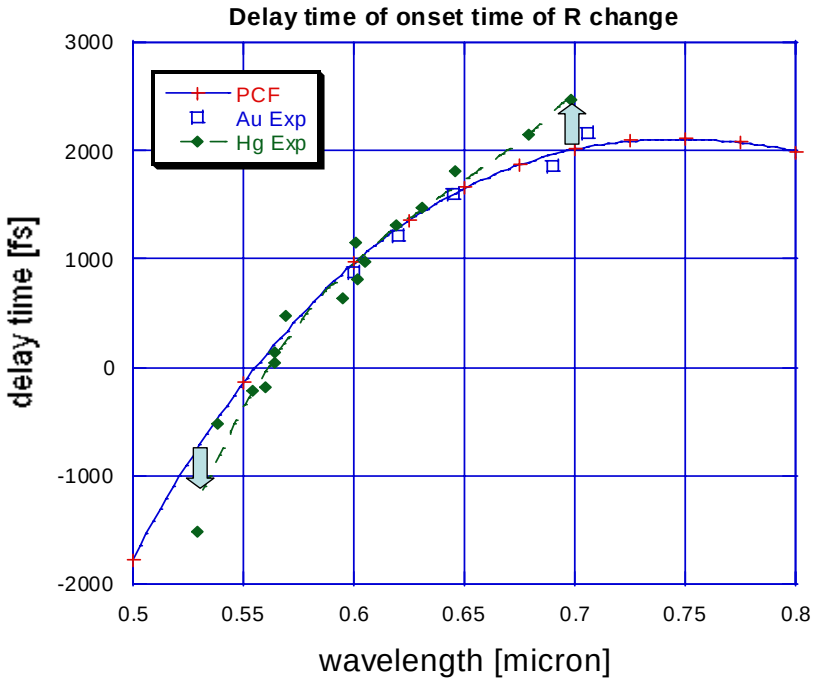

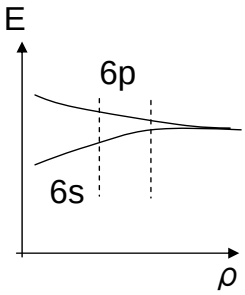

Prepulse effect for High Z target

Blue shift from weak ionized preplasma

Optical pressure compression

P_{laser}=I/c

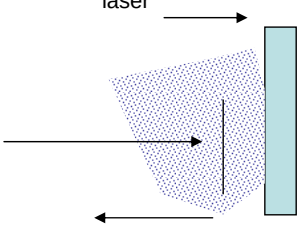

Ionization front

100fsx10^7m/s~1 μ m

~10^{11}W/cm^2

Prepulse energy

~10^{12}W/cm^2
at 12ns before

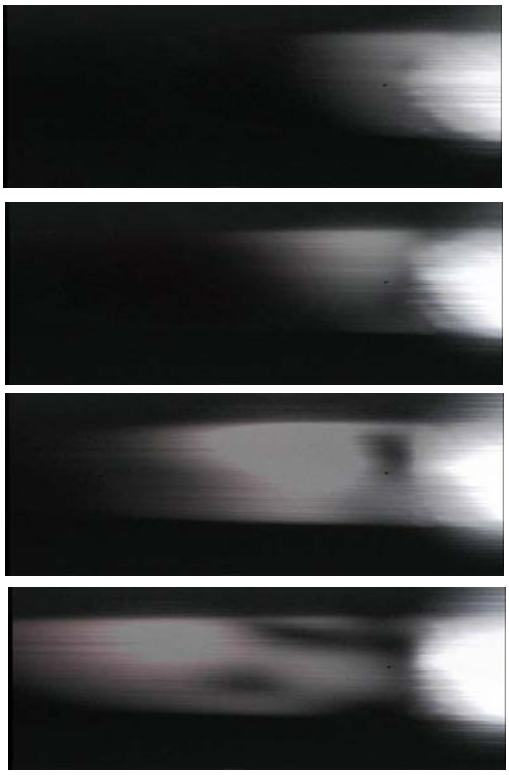

10nm

25nm Doppler shift =>1x10^7m/s

Plasma photonic device: Liquid metal M-NM transition switch

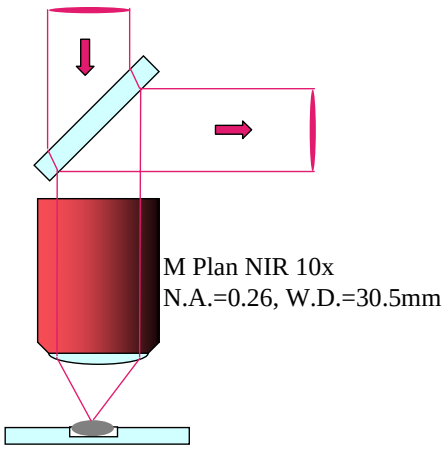

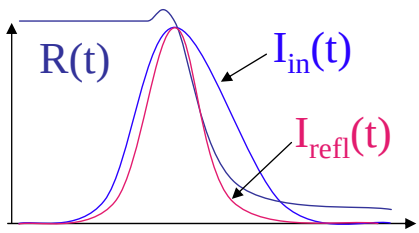

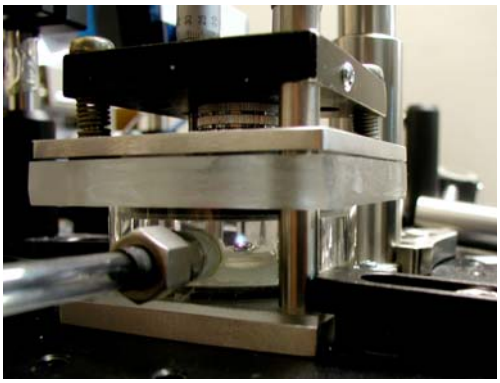

Far-field pattern of reflected laser

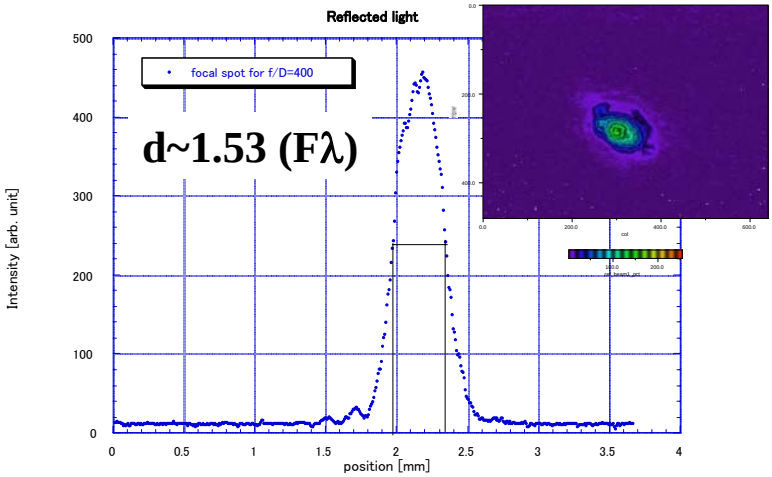

Ultrashort-laser-pulse measurement: Frequency-Resolved Optical Gating (FROG)

$$I_{XFROG}(\omega,\tau) = \left| \int_{-\infty}^{\infty} E(t) E_{gate}(t-\tau) \exp(-i\omega t)\, dt \right|^2$$

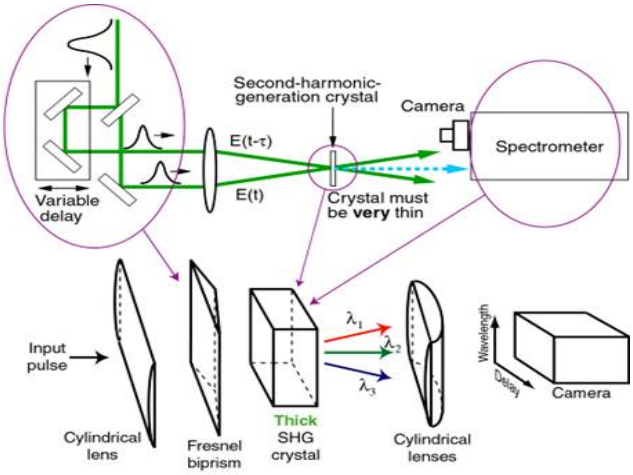

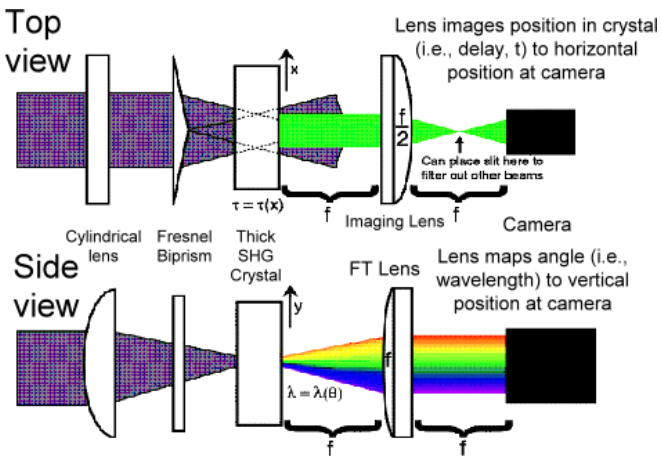

Akturk, S., et al., Opt. Expr., 2003. 11(5): p. 491-501.

Plasma photonic device: FROG results for reflected light

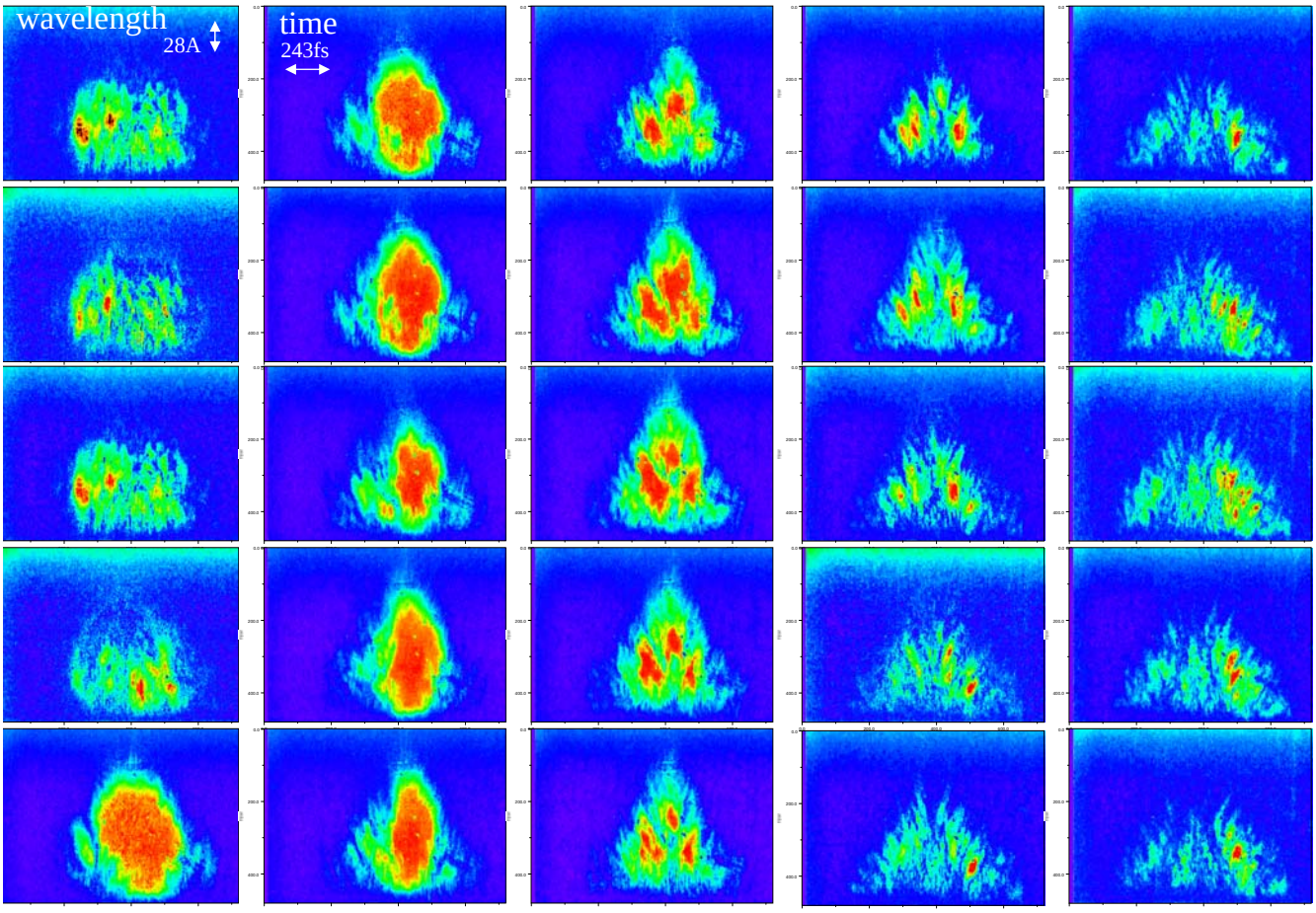

Pulse shortening with saturable absorber switch

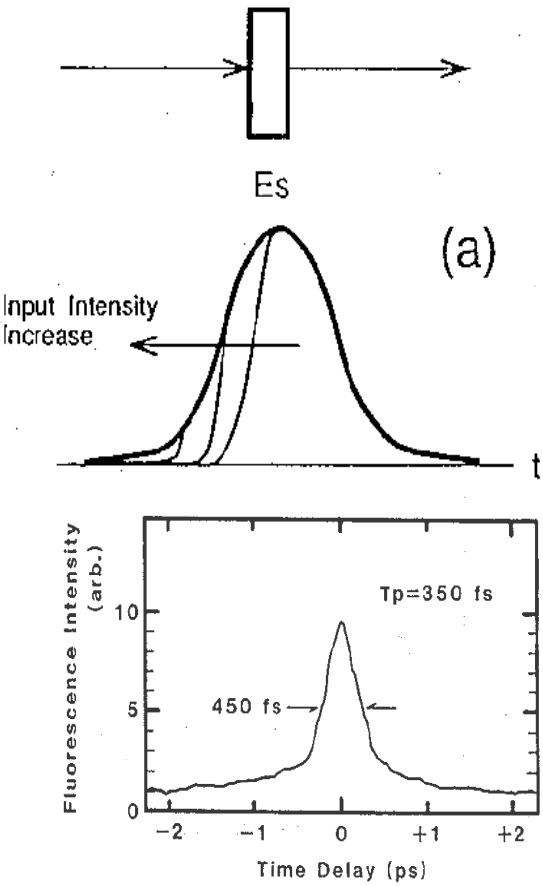

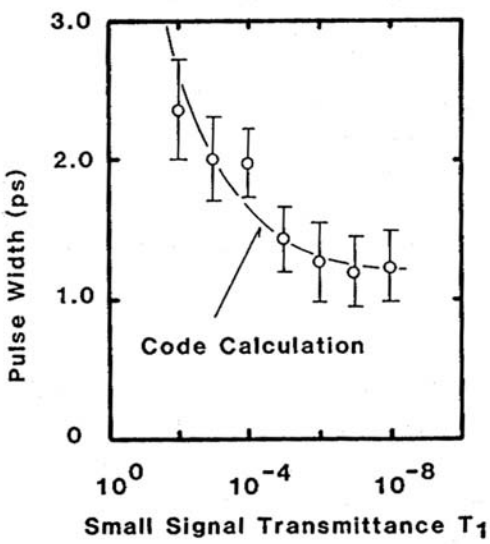

Fig.13 Pulse width of the first pass output vs transmittance of saturable absorber.

UV saturable absorber for short-pulse KrF laser systems
H. Nishioka, H. Kuranishi, K. Ueda, and H. Takuma
Optics Letters, Vol. 14, Issue 13, pp. 692

Other wavelength probe

Interband, intraband transition

Longer wavelength
=>
Drude components check
Extrapolate to DC conductivity

Plasmonic resonance

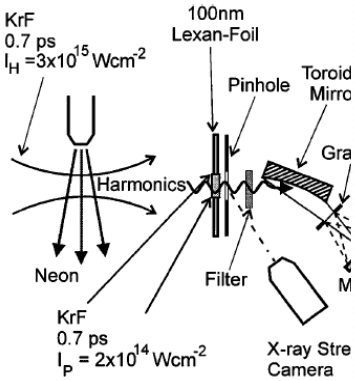

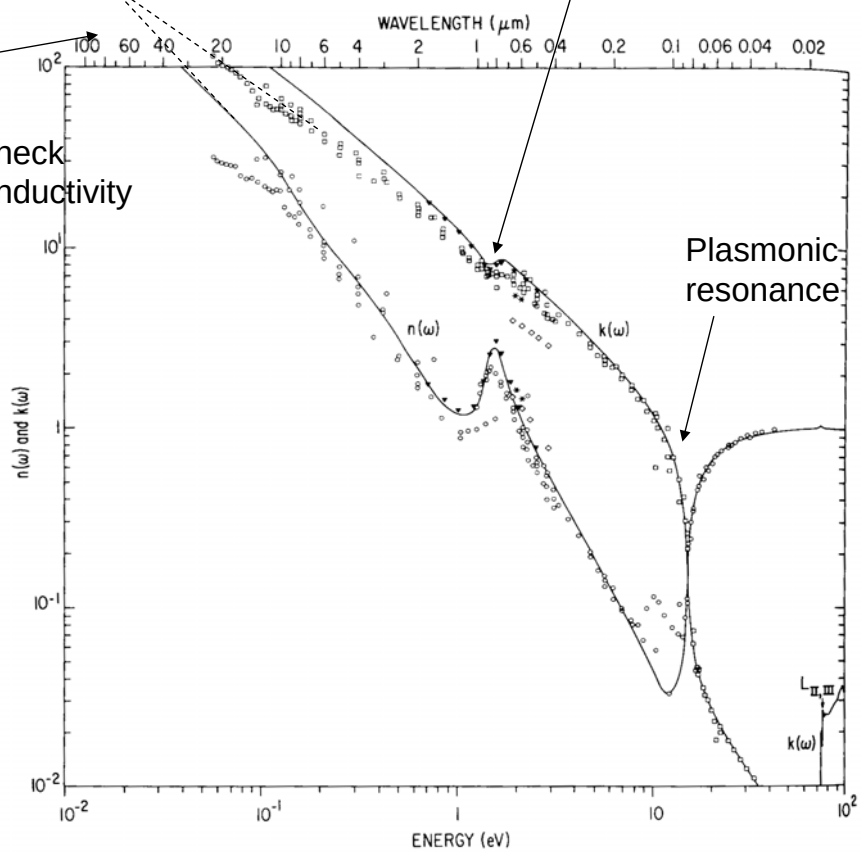

Dynamical and optical properties of warm dense hydrogen

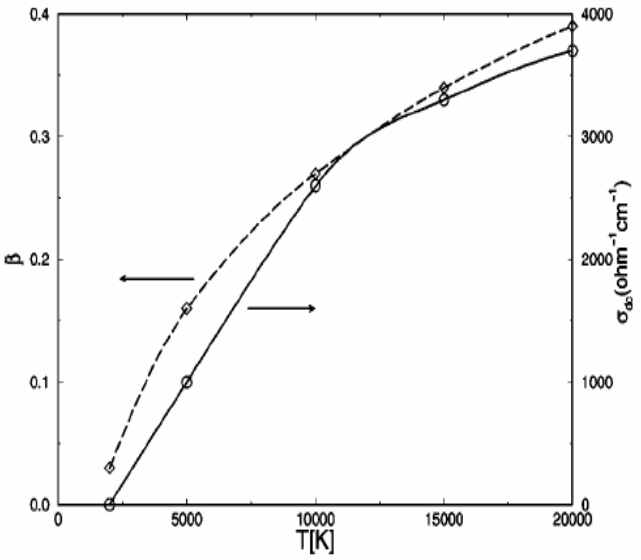

FIG. 10. Comparison of dc electrical conductivity σ_{dc} (solid) and dissociation fraction β (dash) for $r_s = 2$ as a function of temperature.

L.A.Collins, et al., PRB, 63, 184110 (2001)

This is CW heating and slow temperature measurements.
How about highly temporal resolution system?

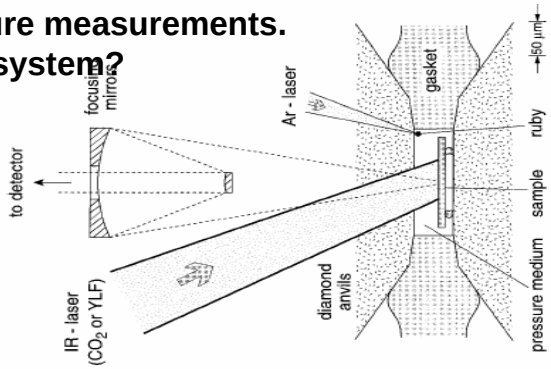

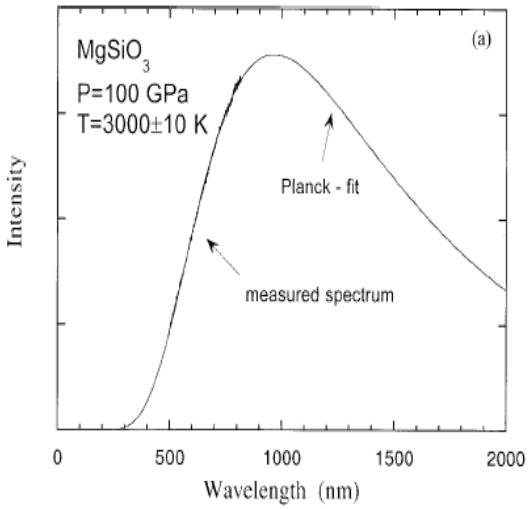

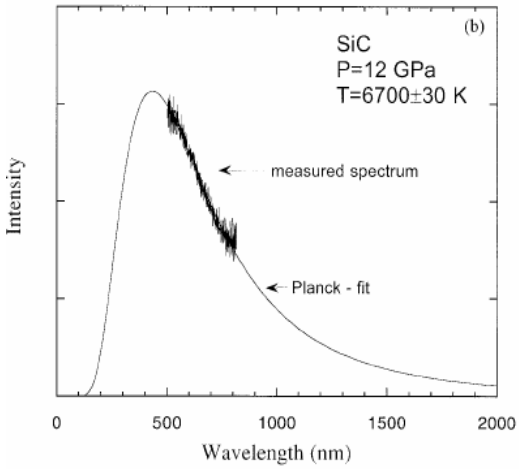

Figure 4. Two examples of temperature measurements at extreme conditions, showing the collected emission spectra and the Planck fits (and fitting error). (a) $MgSiO_3$ is a low-emissivity material heated with a CO_2 laser at 100 GPa. (b) SiC was heated with a CO_2 laser to 6700 K, the highest temperature measured thus far in a diamond cell.

Femtosecond Optically Gated Fluorescence

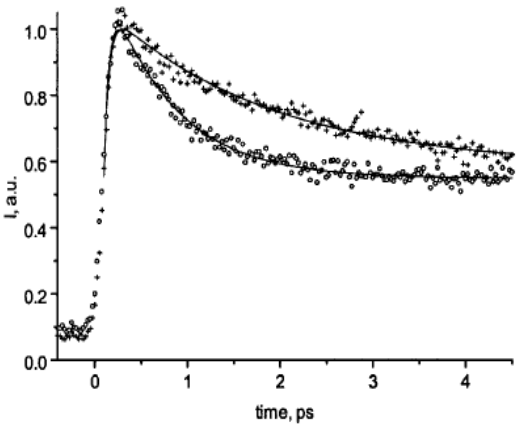

Figure 3. Picosecond fluorescence decay curves for PQ2 in ethanol (+) and in acetonitrile (O). The fittings take into account instrumental response function (~100 fs) and result in lifetimes of 1.8 and 0.7 ps for ethanol and acetonitrile solutions, respectively.

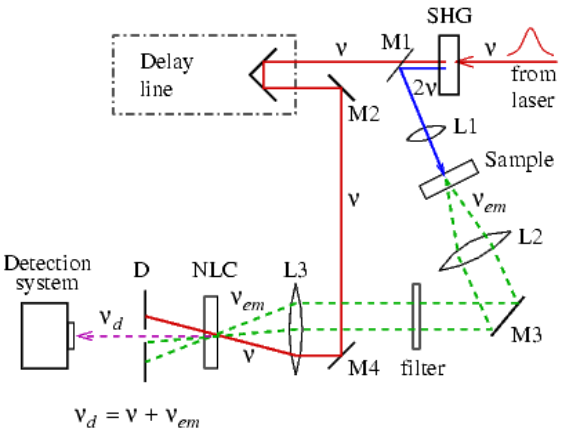

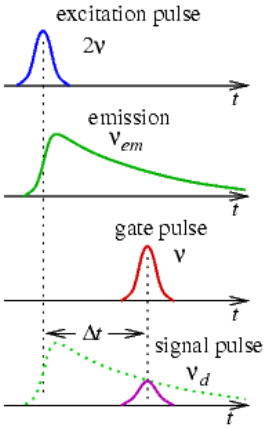

Emissivity of WDM matter?

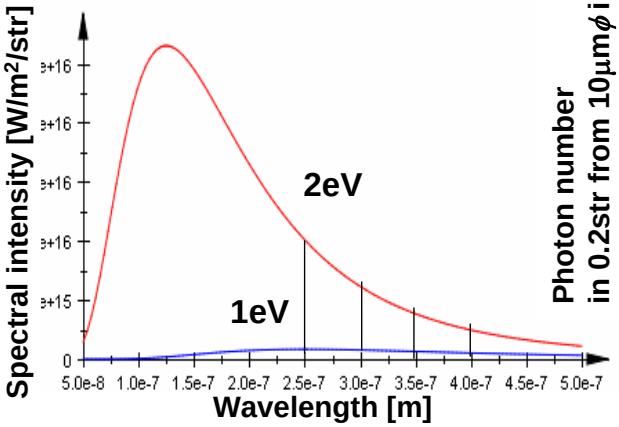

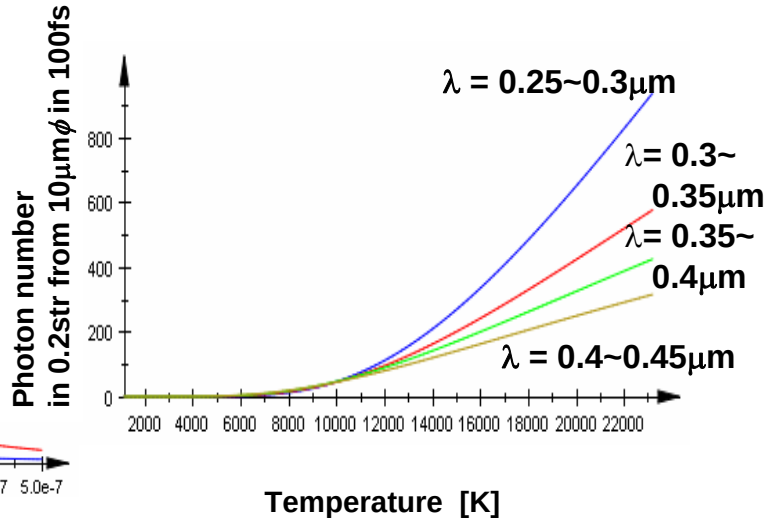

How to measure?
(dt~100fs, dλ~50nm)

1/5str.

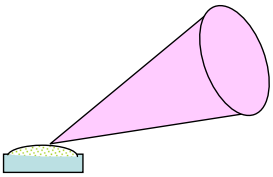

QE~0.1
S/N~6~8e
Dynamic R~1/10
dx x dt ??

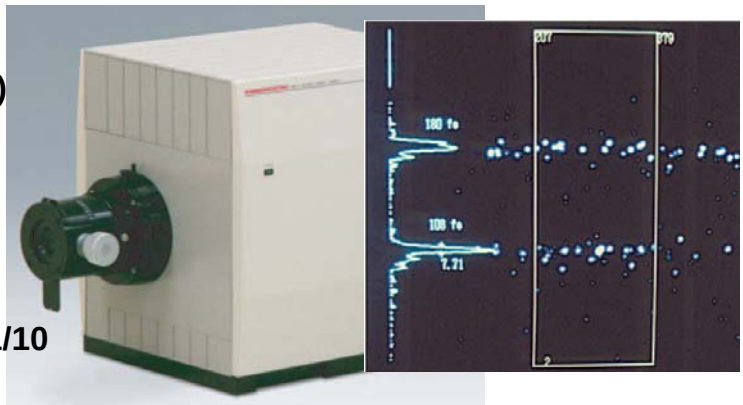

We need new technology for measurements.

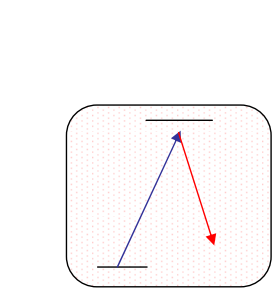

Optical gating?

10^3 *0.1*1.6e-19 ~ 10^{-17}C /10pF*10^3shot~1.6mV

Large coherent medium

Gain should be higher.
Not to require the coherence
Katsuragawa, in UEC-COE

1/5str.

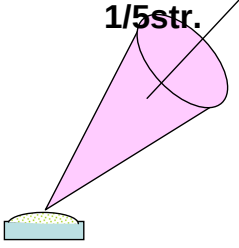

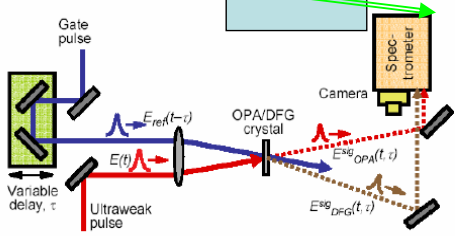

OPA
Gain should be higher.
to need coherence
10mm*f*, 1/5str
=>x 1/6 + temporal phase

10^3photon/100fs
=>480aJ

Fig. 1. Schematic of the experimental apparatus for OPA/DFG XFROG. The gate pulse is characterized using a GRENOUILLE (not shown) before it enters the XFROG setup.

Jing-yuan Zhang, OPT. Express, 11, 601(2003)

Optical CT measurements

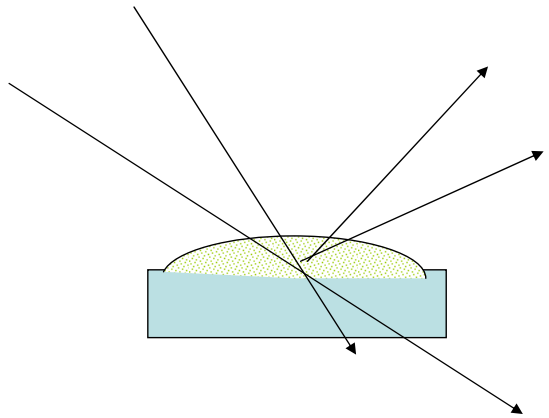

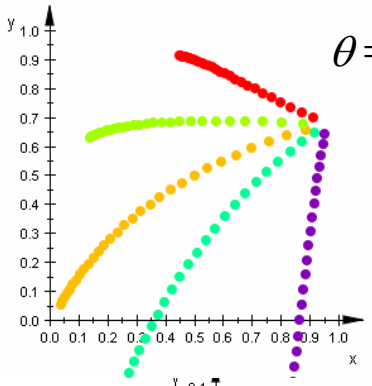

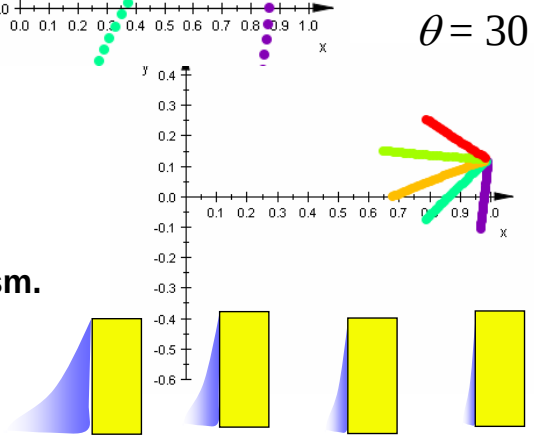

Measured probe is affected by many mechanism.
=> How to solve this Inverse problem?

1 probe => n, k, d
2 probes => n_1, k_1, n_2, k_2, d_1, d_2

Different analytical method?

This is slow measurements of melting but how about dynamics?

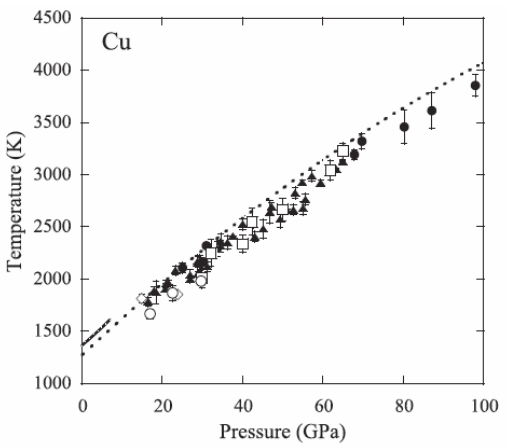

FIG. 2. Melting curve of copper. Experimental data points from this study are shown for various pressure media as open squares (MgO), open circles (CsCl), filled circles (Al_2O_3 disk), filled triangles (1–3 μm Al_2O_3 powder), and open diamonds (nanocrystalline Al_2O_3 powder). Previous experimental work by Akella *et al.* [7(a)] covering the pressure range from 1 atm to 6 GPa is shown as a solid line. The theoretical melting curve from Vocadlo *et al.* [11] is a dotted line.

S. Japel, et al., PRL 95, 167801(2005)

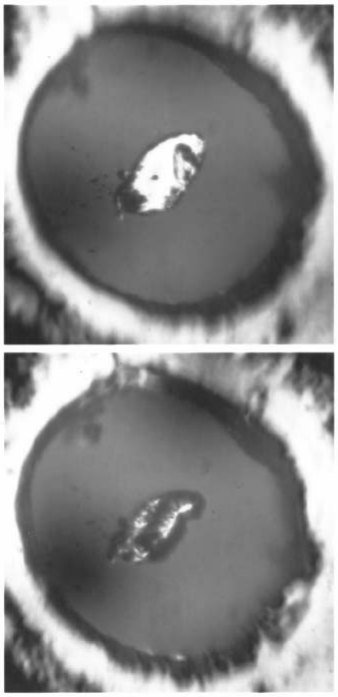

FIG. 1. A Mo sample shown before (top) and after melting (bottom) at 17 GPa.

D. Errandonea, et. al., Phys. Rev. B 63, 132104 (2001)

Au targets were heated to plasma temperature.

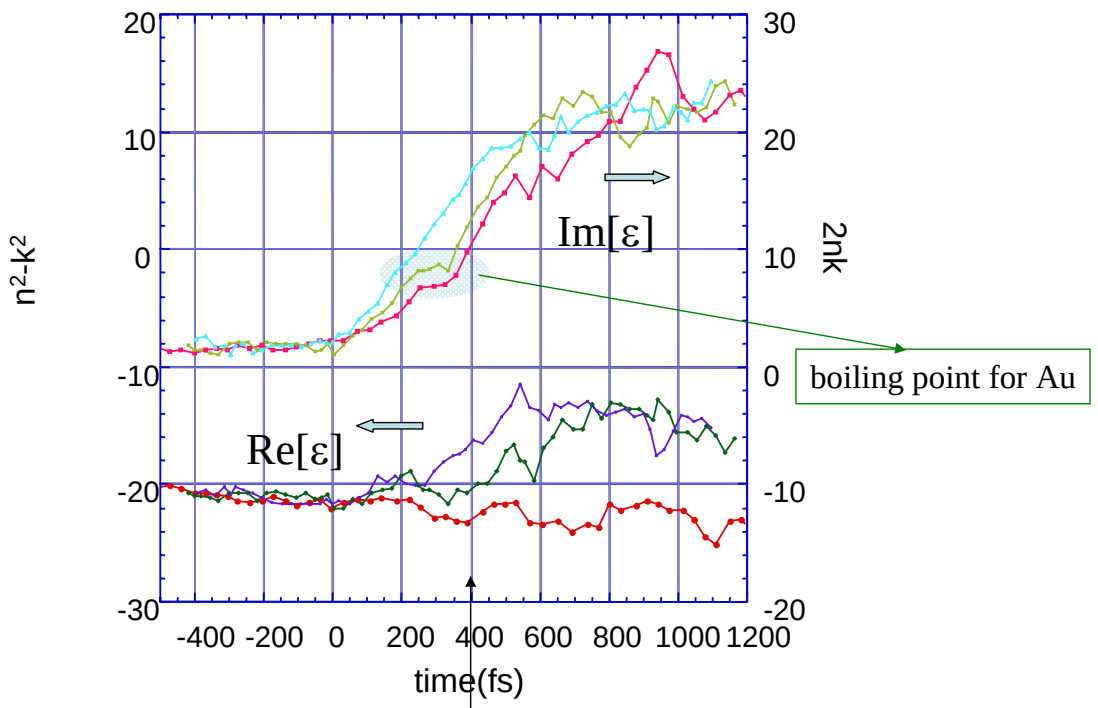

When does expansion occur?

We know it from reconstruction method.

Pump-Pump-probe experiments

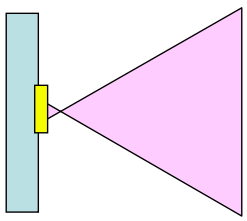

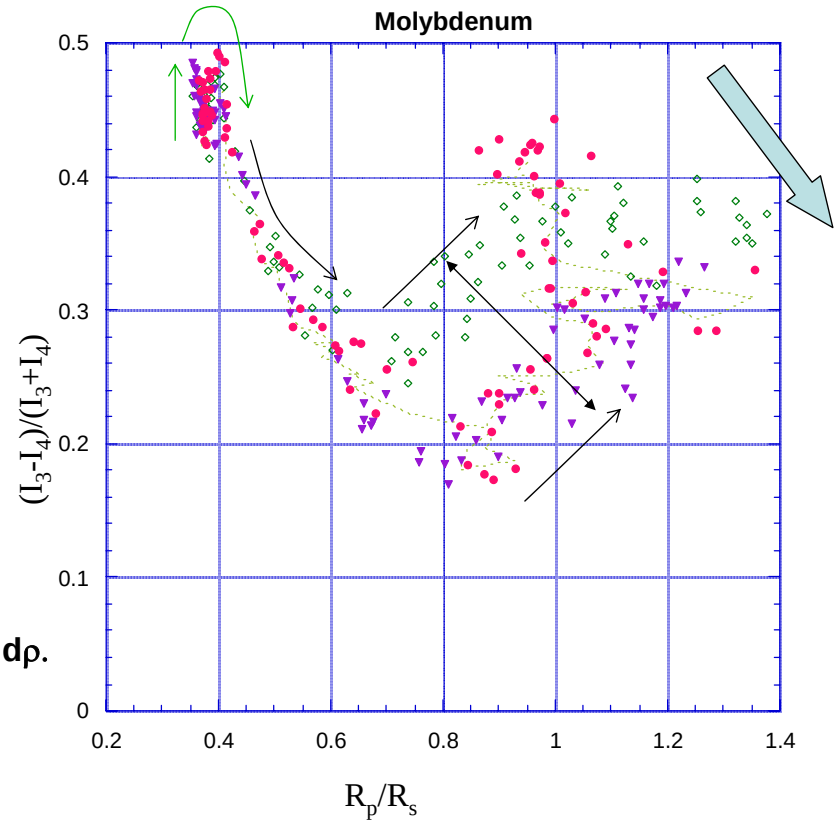

WDM controlling exp.?

Slightly lower density
Small dt may results in big dρ.

We observe regular oscillating refection at late time.

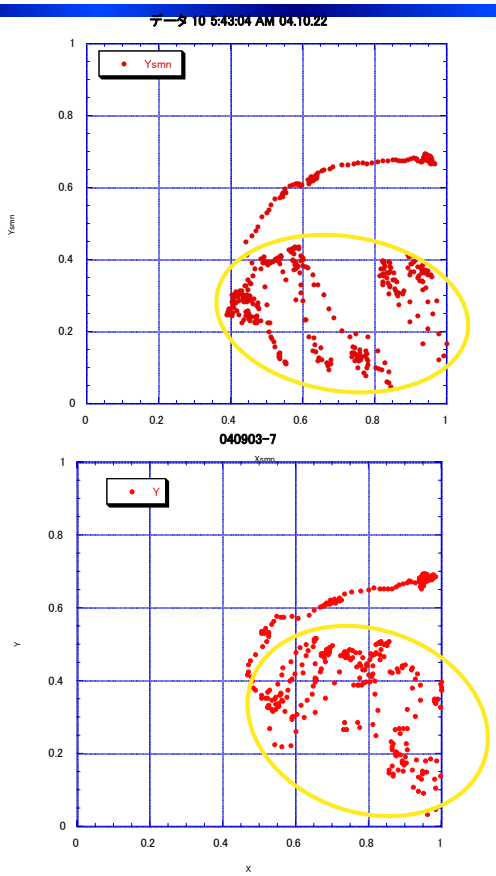

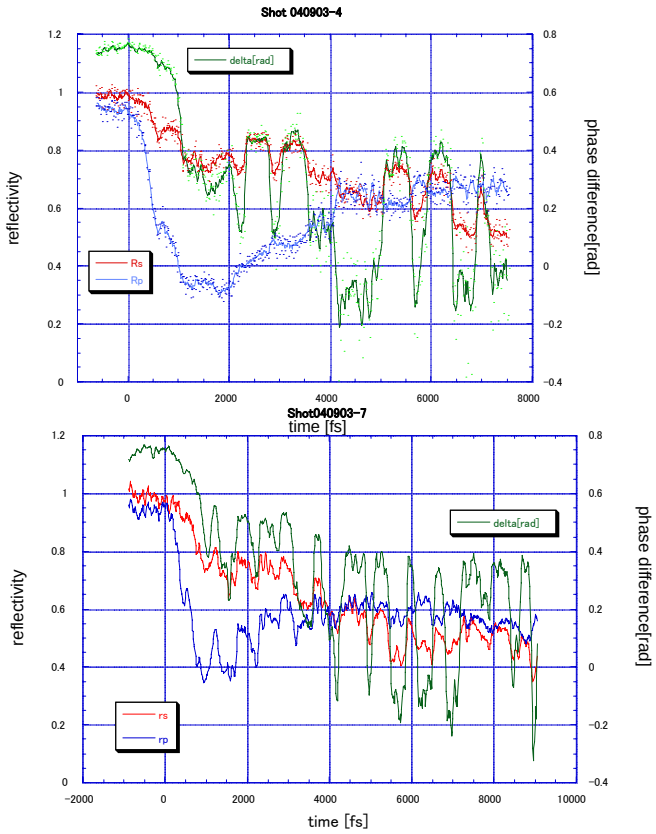

Binary states between transparent and opaque material condition?

Penetration depth of probe beam will suddenly change with some transition.

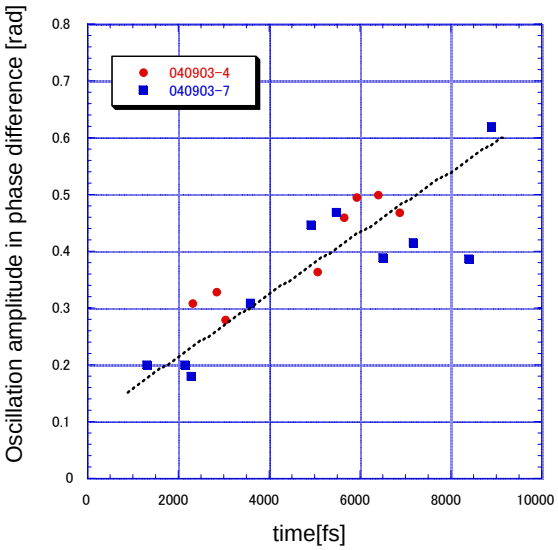

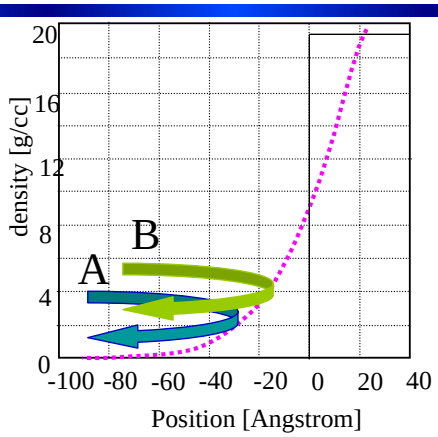

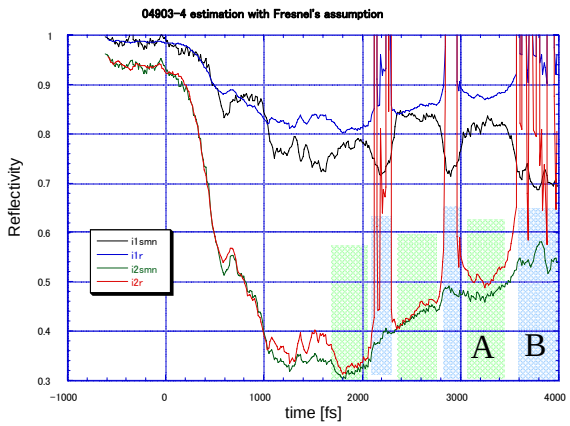

Sound wave detection

Laser drive= laser interferometer detection

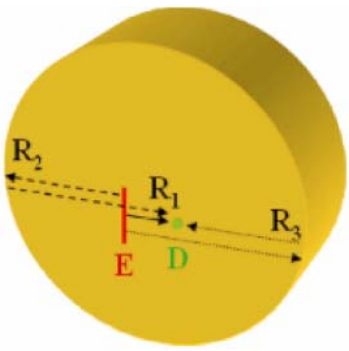

FIG. 6. Scheme of the propagation paths of the RWs in the cylindrical sample: (E) and (D) symbolize the excitation and detection laser beams; R

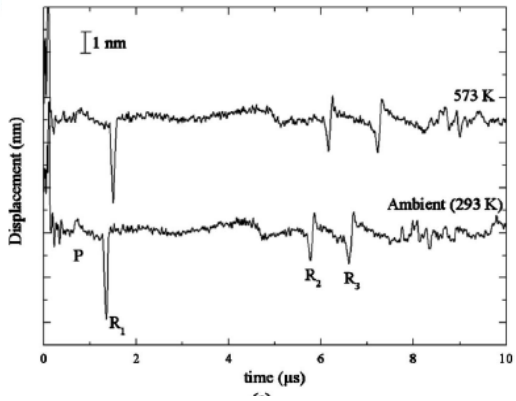

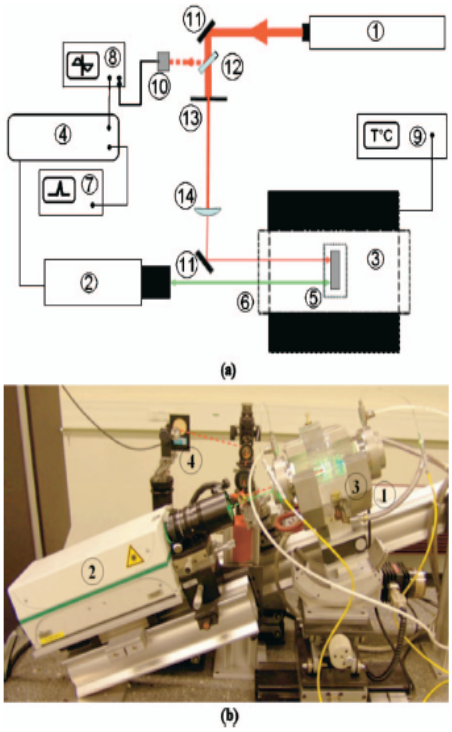

C. Hubert, RSI 78, 024901 (2007)

Sound velocity vs. phase transition

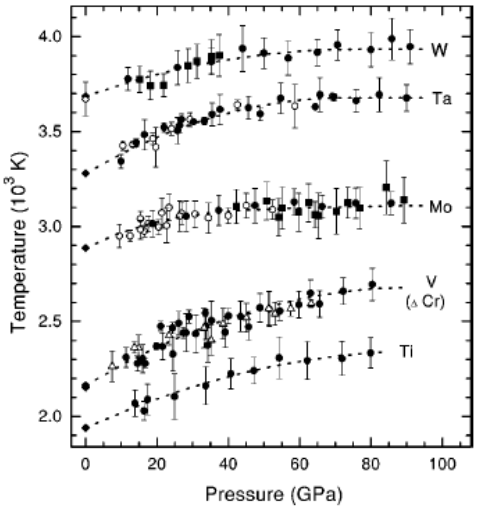

FIG. 2. Melting curves of Mo, Ta, W, V, Ti, and Cr. Solid circles and squares correspond to *in situ* measurements (laser speckle method) in an Ar or Al_2O_3 pressure medium, respectively. Empty circles correspond to the formation of beads as shown in Fig. 1. Open triangles represent the Cr data obtained in situ under Ar. Solid diamonds are 1 atm data. The open diamond represents melting measurements of W in vacuum using identical optics as in the high pressure experiments.

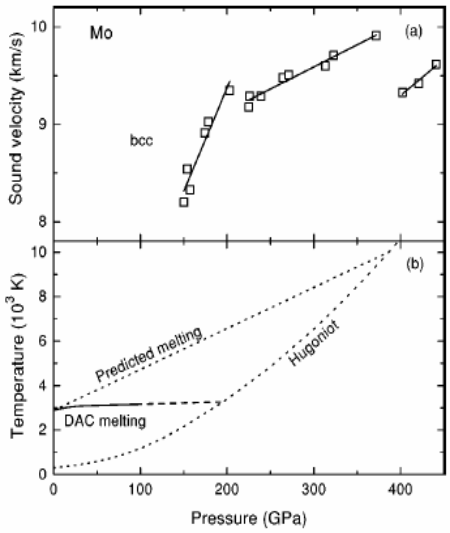

FIG. 3. (a) Experimental sound velocity data of Mo (Ref. 12); (b) DAC melting curve of Mo (solid line), predicted melting curve and Hugoniot temperatures (dotted lines) (Ref. 10). Extrapolation of DAC melting temperatures to higher pressures (dashed line) indicates that the break in sound velocities measured along the Hugoniot at 200 GPa is due to the onset of melting.

Viscosity problems

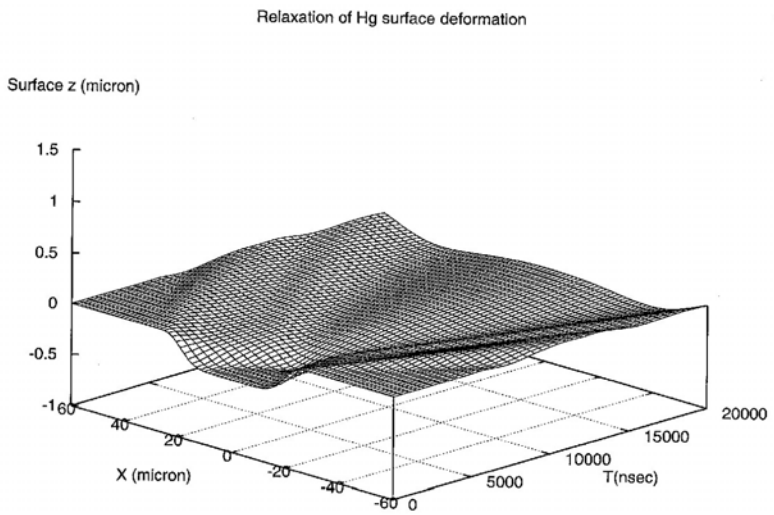

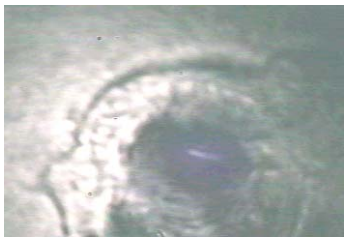

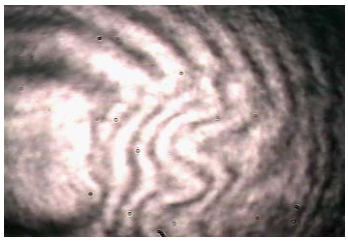

Pump-pump-probe experiments are needed.

Can we measure the DC conductivity?

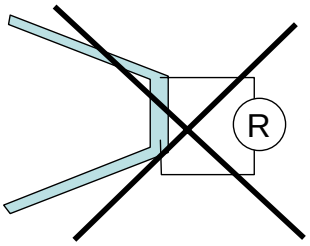

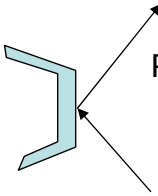

Pump probe with optical frequency

far from DC?

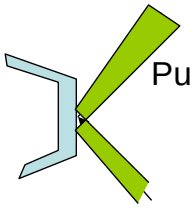

Pump probe with long wavelength (THz)

large effect with low density plasma?

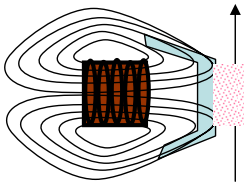

Pulsed B measurements

estimation of ρ?

And some applications we need.

Almost industrial application pass through WDM region.

W may have large polarizability in this frequency

W trajectories 04906&7

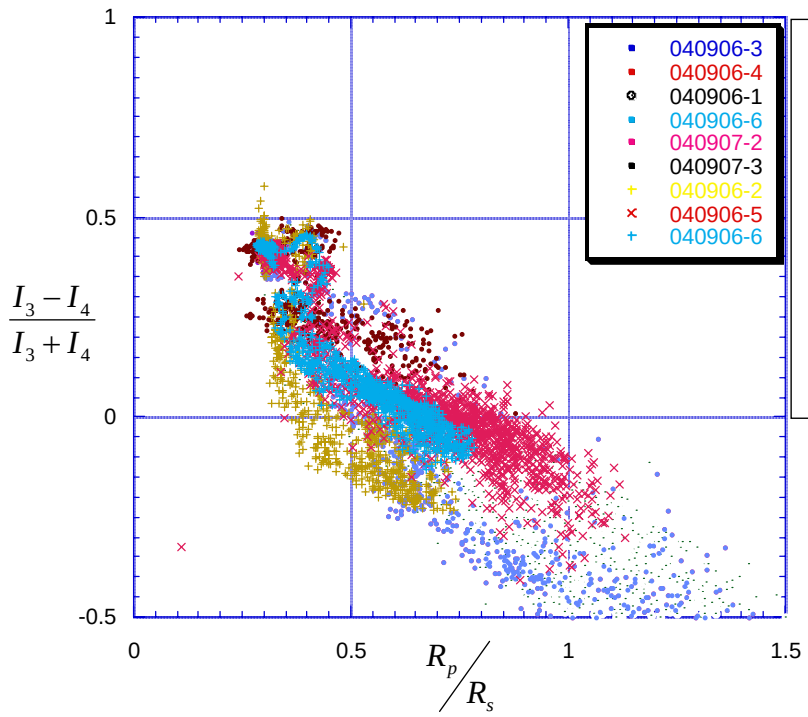

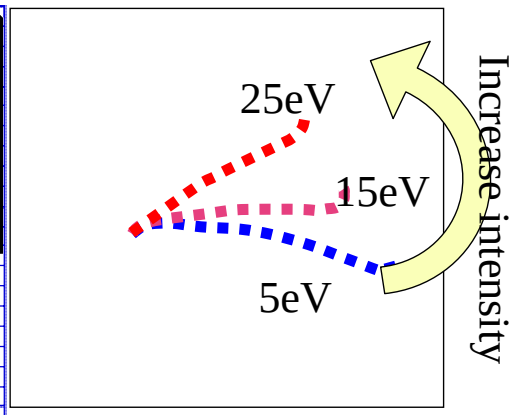

Drude/1000
+(-2600+90i)x10^{-24}cm^3 for WI
+(-1800+200i) x10^{-24}cm^3 for WII